Applied Physics A (2020) 126:304
https://doi.org/10.1007/s00339-020-03476-8

Applied Physics A
Materials Science & Processing

S.I. : CURRENT STATE-OF-THE-ART IN LASER ABLATION

Expansion of laser-induced plume after the passage of a counter shock wave through a background gas

Akira Higo[1] · Keita Katayama[1] · Hiroshi Fukuoka[2] · Takehito Yoshida[3] · Tamao Aoki[4] · Minoru Yaga[5] · Ikurou Umezu[4]

Received: 15 October 2019 / Accepted: 18 March 2020 / Published online: 31 March 2020

Abstract
Double-pulsed laser ablation with two targets and lasers in a background gas is a method to form nanoparticle complex. Effects of pulse delay between two lasers on plume expansion dynamics are discussed. The germanium and silicon targets were set parallel to each other and irradiated by two YAG lasers. The germanium target was irradiated followed by irradiation of the silicon target with delay time, t_d. We found that the expansion distance of delayed silicon plume is enhanced for $2\ \mu s \le t_d \le 50\ \mu s$, compared to that when only the silicon target is irradiated. For $t_d = 200\ \mu s$, the expansion distance of delayed silicon plume is similar to that when only the silicon target is irradiated. We discuss the expansion dynamics of the delayed silicon plume based on the effect of the density distribution induced by the primary germanium plume. Our results indicate that the effect of primary germanium plume remains up to about $t_d = 50\ \mu s$, and it disappears by $t_d = 200\ \mu s$.

Keywords Pulsed laser ablation · Shock wave · Plume expansion · Pulsed laser deposition

1 Introduction

It is well-known that the pulsed laser ablation (PLA) in a background gas is one of the dry processes to prepare nanoparticles. The predominant feature of PLA is non-equilibrium temporal and spatial evolutions of the plume. Gas-phase plume changes to nanoparticles by collisional processes during the expansion in a background gas [1, 2]. The morphology of nanoparticle aggregates deposited on the substrate varies with PLA condition due to the temporal and spatial distribution of nanoparticles in the plume [3, 4]. The double-pulsed laser ablation (D-PLA) is a method to provide a new growth field of nanoparticles induced by the collision of two plumes [5–10]. The interaction of two laser-induced plumes is also important for laser-induced breakdown spectroscopy (LIBS). The enhancement of plume intensity by the interaction of two plumes is reported [11–14], and this technique is used to increase the detection limit of LIBS. Not only in the field of pulsed laser ablation [15–18], but the collision of expanding plasma is also important in many research fields. There are extensive reports from viewpoints of laboratory simulations of astrophysical plasmas, design of inertial confinement fusion Hohlraums, and so on [19–22]. We previously observed the backward motion of the plume due to the collision with the counter shock wave when two targets are irradiated simultaneously [6]. Many of the previous researches are discussed on the collision during the simultaneous plume expansion. Collision of the plume with delay will modify the growth and aggregation processes of nanoparticles. The effects of pulse delay applied to the second laser pulse on the expansion dynamics of the delayed plume are discussed in the present paper.

2 Experiment

A block diagram of our D-PLA system is shown in Fig. 1. Silicon and germanium targets were set parallel to each other and irradiated by two YAG lasers. The excitation

✉ Ikurou Umezu
umezu@konan-u.ac.jp

[1] Graduate School of Natural Science, Konan University, Kobe 658-8501, Japan

[2] National Institute of Technology, Nara College, Nara 639-1080, Japan

[3] National Institute of Technology, Anan College, Anan 774-0017, Japan

[4] Department of Physics, Konan University, Kobe 658-8501, Japan

[5] Department of Mechanical System Engineering, University of the Ryukyus, Nishihara 903-0213, Japan

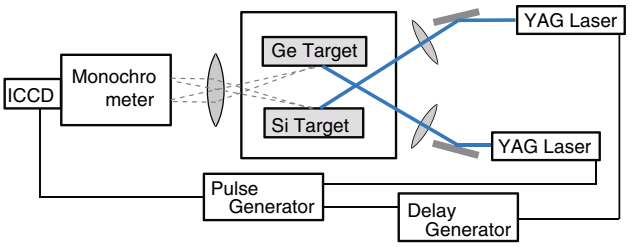

Fig. 1 Block diagram of the experimental setup for D-PLA

wavelengths of two Nd:YAG lasers for silicon and germanium targets were 355 nm and 266 nm, respectively. There is no specific reason for the difference in wavelength. The intensity ratio of two laser powers was set so that the sizes of germanium and silicon plumes are comparable. The laser fluence was roughly estimated by ablated area of the target for a laser pulse, and estimated values for silicon and germanium targets were about 5 and 8 J/cm^2, respectively. The distance between the targets was 9 mm. Helium gas was introduced in a chamber as a background gas, and the gas pressure was kept at 500 Pa. Plume expansion dynamics were monitored through plasma emission intensity of the plume measured by a gated ICCD camera equipped with a monochrometer. The plume emission intensity was measured along the line between laser focusing points on the silicon and germanium targets. Monochromatized silicon or germanium emission lines were selected to observe the emission intensity of each species. We define the plume edge as the position where the plume intensity is a half value of the maximum intensity. This plume edge corresponds to the contact front between the plume and background gas. An example of plume emission image and plume emission intensity, when only the silicon target is irradiated, is shown in Fig. 2. In the present paper, the germanium target was irradiated followed by irradiation of the silicon target with delay time, t_d. We name PLA with a target and a laser as single PLA (S-PLA) and that with two targets and two lasers as double-PLA (D-PLA) in the present paper.

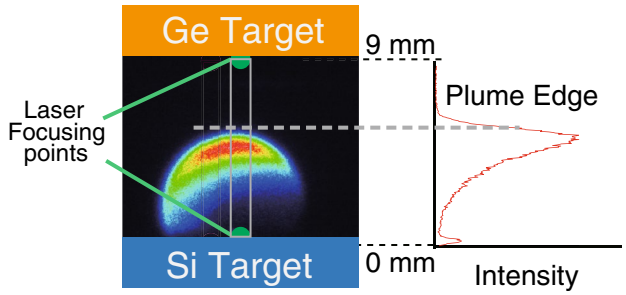

Fig. 2 An example of plume image and emission intensity distribution measured by ICCD camera. Plume emission was analyzed along the rectangle in the figure. Plume edge is defined as the position where the plume intensity is a half value of the maximum intensity

3 Results

The time evolution of the plume edges for S-PLA of germanium and silicon targets is shown by circles in Fig. 3a, b, respectively. Silicon and germanium targets are at positions of 0 and 9 mm, and the plumes expand toward 9 and 0 mm, respectively. It is well-known that the position of the shock front as a function of time, $R(t)$, is described as follows for point blast expansion:

$$R(t) = \xi_0 \left(E_0/\rho_a\right)^{1/5} t^{2/5}. \quad (1)$$

Here ξ_0 is a constant, E_0 is the initial energy of the plume, and ρ_a is the density of gas ahead of shock wave [23]. Since E_0 corresponds to incident laser energy in our experimental setup and is constant value, the value of $\xi_0(E_0/\rho_a)^{1/5}$ in Eq. (1) is determined by ρ_a. The value of ρ_a is the density of the background helium gas for S-PLA. The experimental results were fitted to the following equation:

$$R(t) = Ct^n. \quad (2)$$

The broken lines in Fig. 3 are the best-fitted lines up to 0.5 μs, and the best-fit values of n are about 0.40 and 0.43 for silicon and germanium targets, respectively. These values are close to the value of 2/5 in Eq. (1). This indicates that expansion dynamics is well-described by the point blast model and fitted lines correspond to the expansion distance of the shock front. The shock front gradually separates from the plume edge [24] after 0.5 μs.

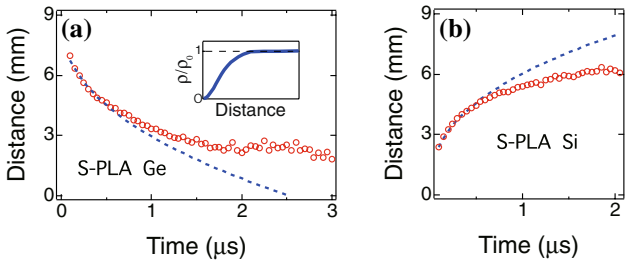

Fig. 3 Results of S-PLA when **a** germanium and **b** silicon targets are irradiated. Positions of plume edge (circles) and estimated shock front (broken lines) are shown as a function of time. Germanium and silicon targets are set at 9 and 0 mm, respectively. An inset in **a** is a schematic view of the final density distribution after the shock wave weakened and changed to the sound wave. Here, ρ_0 is the density of background gas. The origin of the distance in the inset is not the same as that of the main figure of **a** but the center of the point blast expansion

The results of D-PLA for $t_d = 5$ and 200 μs are shown in Fig. 4a, b, respectively. Crosses show the plume edge of D-PLA, and the circles are the same as those in Fig. 3b. The times in these figures are the times after the irradiation of silicon target. The emission of the primary germanium plume attenuates and is hardly observed for these delay times. For $t_d = 200$ μs, the expansion of silicon plume is quite similar to that of S-PLA as shown in Fig. 4b. For $t_d = 5$ μs, we can observe an enhancement of the plume expansion distance compared with that of S-PLA after about 0.3 μs, as shown in Fig. 4a. A similar enhancement is observed for $2\ \mu s \le t_d \le 50\ \mu s$ (not shown in the figures) and is not observed for $t_d \ge 200$ μs, while the plume expansion distance is almost the same with that of S-PLA up to about 0.3 μs regardless of the value of t_d. We consider the origin of enhancement of plume expansion distance by using results for $t_d = 5$ μs in the next section because the large enhancement is observed at around this time delay.

4 Discussion

The result of Fig. 3a indicates that the shock front induced by primary germanium plume passes through the space between targets before the irradiation of silicon target when $t_d \ge 2.5$ μs. This means that delayed silicon plume expands not in the original helium background gas for $t_d = 5$ μs. Therefore, the enhancement of plume expansion distance in Fig. 4a should be due to the primary germanium plume. Since the plume expansion for $t_d = 200$ μs is similar to that of S-PLA, the effect of germanium plume disappears by this time region.

One of the possible origins of the enhancement of plume expansion distance is the effect of the reflected shock wave at the surface of the silicon target, as discussed in the double-pulse pre-ablation configuration [11, 13]. The low-density region near the silicon target induced by the reflected shock wave will enhance plume intensity. However, it is difficult to explain the feature of the expansion, shown in Fig. 4a, by the effect of the reflected shock wave. It is considered that the effect of the reflected shock wave will decrease with time (distance from the silicon target). Nevertheless, enhancement is not observed at less than 0.3 μs (up to 4 mm from the silicon target) and observed at a later stage. Since the Mach number of the shock front, M, when the shock wave reaches the surface of the counter target is $M \sim 1.5$ in our experimental condition and $M \ge 2.2$ in Ref. [17], the effect of reflected shock wave may be weaker in our condition.

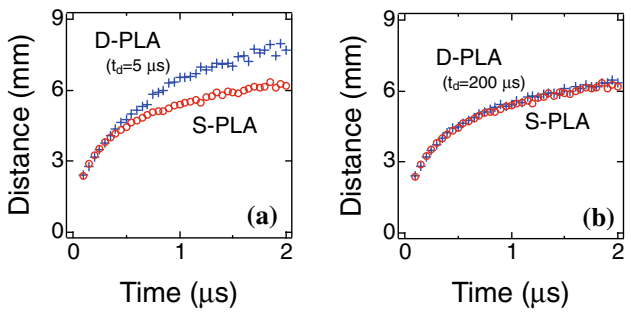

Fig. 4 Results of D-PLA. Crosses show the position of silicon plume edge as a function of time after the irradiation of silicon target for **a** $t_d = 5$ μs and **b** 200 μs. Circles are the result of S-PLA, which is the same as in Fig. 3b

The other possible origin is the change in the density distribution after the shock front passes through the space between targets. The density distribution after the point blast explosion is reported in previous reports [23, 25, 26]. After the shock wave weakened and changed to the sound wave, the final density of the gas far from the explosion center is almost the same as the density of the background gas, and it decreases toward the center as schematically shown in the inset in Fig. 3a. If the effect of reflected shock wave is negligibly weak, a qualitatively similar density distribution is expected when t_d is not small. The delayed silicon plume travels from right to left in the density distribution shown in the inset in Fig. 3a. Note that the origin of the distance in the inset is the center of point blast expansion and not the same as that of the main figure. We consider the result of Fig. 3a based on the density distribution induced by germanium plume.

The expansion dynamics of the shock front depends on the density ahead of the shock front, as shown in Eq. (1). The background helium gas ahead of the shock front uniformly distributes for S-PLA. On the other hand, the delayed silicon plume expands in the gas flow field having non-uniformly distributed density formed by the primary germanium plume. Since both the plume expansions of S-PLA and D-PLA for $t_d = 5$ μs obey Eq. (1) up to 0.3 μs, expansion dynamics of D-PLA is equivalent to that of the S-PLA in this time region. The enhancement of plume expansion is observed after 0.3 μs. As well as the shock front, the expansion dynamics of the plume edge depends on the density ahead of the plume edge. Since the position of silicon plume edge at 0.3 μs is about 4 mm, the experimental results shown in Fig. 4a can be explained by assuming that the gas density ahead of the shock front is similar to that of the original helium background gas up to about 4 mm and is lower to that above about 4 mm.

A similar enhancement is observed for $2\ \mu s \le t_d \le 50\ \mu s$ and not observed for $t_d \ge 200$ μs. These results suggest that the effect of germanium plume disappears due to the replacement with the original helium gas by diffusion or formation of germanium nanoparticles for $t_d \ge 200$ μs. The value of $t_d = 200$ μs is consistent with the previous reports that the formation of silicon nanoparticles in the background

gas starts on the order of a few hundred microseconds [2, 27]. Our experimental results indicate that change in the gas condition ahead of the shock front is significant for D-PLA with pulse delay and suggest that moderate pulse delay will give a new growth field. If the origin of the similar expansion dynamics between D-PLA for $t_d = 200$ μs and S-PLA is due to the formation of germanium nanoparticles, growth of silicon in a mixture field with germanium nanoparticle and silicon plume might be possible.

5 Conclusions

The germanium target was irradiated followed by irradiation of the silicon target at delay time, t_d. We found that the expansion distance of delayed silicon plume is enhanced for $2\ \mu s \leq t_d \leq 50\ \mu s$ compared to that when only the silicon target is irradiated, while this enhancement is not observed for $t_d \geq 200$ μs. The origin of this enhancement is that the delayed silicon plume expands in the gas flow field after the shock wave induced by primary germanium plume passes through the space between targets. The effect of primary germanium plume on the delayed silicon plume disappears by $t_d = 200$ μs. The expansion dynamics of delayed silicon plume can be explained by taking into account the change in the density distribution caused by the primary germanium plume.

Acknowledgements This work was partially supported by JSPS KAKENHI Grant No. JP19K03815.

References

1. T. Yoshida, S. Takeyama, Y. Yamada, K. Mutoh, Appl. Phys. Lett. **68**(13), 1772 (1996)
2. D.B. Geohegan, A.A. Puretzky, G. Duscher, S.J. Pennycook, Appl. Phys. Lett. **72**, 2987 (1998)
3. I. Umezu, A. Sugimura, M. Inada, T. Makino, K. Matsumoto, M. Takata, Phys. Rev. B **76**, 666 (2007)
4. T. Yoshida, N. Yagi, R. Nakagou, A. Sugimura, I. Umezu, Appl. Phys. A **117**, 223 (2014)
5. Y.K. Jo, S.B. Wen, J. Phys. D **44**, 305301 (2011)
6. K. Katayama, Y. Horai, H. Fukuoka, T. Kinoshita, T. Yoshida, T. Aoki, I. Umezu, Appl. Phys. A **124**, 045328 (2018)
7. T. Kinoshita, H. Fukuoka, I. Umezu, Mater. Sci. Forum **910**, 96 (2018)
8. I. Umezu, Y. Hashiguchi, H. Fukuoka, N. Sakamoto, T. Aoki, A. Sugimura, Appl. Phys. A **122**, 485 (2016)
9. I. Umezu, N. Sakamoto, H. Fukuoka, Y. Yokoyama, K. Nobuzawa, A. Sugimura, Appl. Phys. A **110**, 629 (2012)
10. I. Umezu, S. Yamamoto, A. Sugimura, Appl. Phys. A **101**, 133 (2010)
11. G. Cristoforetti, S. Legnaioli, L. Pardini, V. Palleschi, A. Salvetti, E. Tognoni, Spectrochim. Acta Part B **61**, 340 (2006)
12. P.K. Diwakar, S.S. Harilal, J.R. Freeman, A. Hassanein, Spectrochim. Acta Part B **87**, 65 (2013)
13. E. Tognoni, G. Cristoforetti, J. Anal. Atom. Spectrom. **29**, 1318 (2014)
14. X. Li, Z. Yang, J. Wu, J. Han, W. Wei, S. Jia, A. Qiu, J. Appl. Phys. **119**, 133301 (2016)
15. P. Hough, C. McLoughlin, S.S. Harilal, J.P. Mosnier, J.T. Costello, J. Appl. Phys. **107**, 024904 (2010)
16. C. Sánchez-Aké, D. Mustri-Trejo, T. García-Fernández, M. Villagran-Muniz, Spectrochim. Acta Part B **65**, 401 (2010)
17. K.F. Al-Shboul, S.S. Harilal, S.M. Hassan, A. Hassanein, J.T. Costello, T. Yabuuchi, K.A. Tanaka, Y. Hirooka, Phys. Plasmas **21**, 013502 (2014)
18. K.F. Al-Shboul, S.M. Hassan, S.S. Harilal, Plasma Sources Sci. Technol. **25**, 065017 (2016)
19. Y. Hirooka, H. Sato, K. Ishihara, T. Yabuuchi, K.A. Tanaka, Nucl. Fusion **54**, 022003 (2014)
20. R.A. Smith, J. Lazarus, M. Hohenberger, A. Marocchino, J.S. Robinson, J.P. Chittenden, A.S. Moore, E.T. Gumbrell, M. Dunne, Plasma Phys. Control Fusion **49**, B117 (2007)
21. M. Villagran-Muniz, H. Sobral, R. Navarro-González, P.F. Velázquez, A.C. Raga, Plasma Phys. Control Fusion **45**, 571 (2003)
22. P. Velarde, D. García-Senz, E. Bravo, F. Ogando, A. Relaño, C. García, E. Oliva, Phys. Plasmas **13**, 092901 (2006)
23. Y.B. Zeldovich, Y.P. Raizer, *Physics of Shock Waves and High-Temperature Hydrodynamic Phenomena* (Academic Press, New York, 1966)
24. D. Bäuerle, *Laser Processing and Chemistry* (Springer, Berlin, 2000)
25. H.L. Brode, J. Appl. Phys. **26**, 766 (1955)
26. Z. Yang, J. Wu, W. Wei, X. Li, J. Han, S. Jia, A. Qiu, Phys. Plasmas **23**, 083523 (2016)
27. J. Muramoto, T. Inmaru, Y. Nakata, T. Okada, M. Maeda, Appl. Phys. Lett. **77**, 2334 (2000)